Noncollocated Point Control of Nondispersive Distributed-Parameter Systems Using Time Delays

Firdaus E. Udwadia

Mechanical and Civil Engineering Department
University of Southern California
430K Olin Hall
Los Angeles, California 90089-1453

Transmitted by Robert Kalaba

ABSTRACT

This paper deals with the noncollocated, time-delayed active point control of continuous systems. It considers systems of finite spatial extent which can be modeled by the undamped wave equation. The paper presents a new method of control of the system using noncollocated sensors and actuators. By using the physical properties of the mode shapes of vibration of the system it is shown that the modal response at a given location in the system can be reconstructed from the *time-delayed* modal responses at (at most) three different locations in the system. This result is then used to motivate a closed-loop control design which is capable of stabilizing the system and dampening the vibrations in all its modes, using dislocated sensor and actuator locations. It is found that the cost of dislocating the sensors from the actuator is at most an additional two sensors. For special types of boundary conditions this cost may be reduced to one additional sensor, or even be completely eliminated. Simple finite-dimensional controllers, commonly used in control design, are found to suffice. The results are valid for rather general conditions at the boundaries of the continuum. Explicit conditions are provided to obtain the bounds on the controller gains to ensure stability of the closed-loop control design. These bounds are obtained in terms of the locations of the sensors and the actuators. Simulation results, which validate the control methodology and the theoretical bounds on the gain, are also presented.

INTRODUCTION

The control of distributed systems is an active area of current research. It has wide-ranging applications in the fields of aerospace engineering, mechanical engineering, civil engineering, and petroleum engineering. The control

of large space structures for vibration suppression and pointing controls, the control of rotors and shafts and mechanical assemblies, active control of buildings subjected to earthquakes, and the control of oil recovery from natural reservoirs are some examples (see for example [4, 5, 2, 9, 7, 10, 1, 13, 14, 15]).

In this paper we consider systems which are of finite spatial extent and which can be modeled by the one-dimensional undamped wave equation. The boundary conditions are taken to be homogeneous and unmixed. We show that noncollocated point control of such a neutrally stable distributed system, using finite-dimensional controllers, can lead to complete controllability of the system without any spillover effects. Furthermore, it is shown that a large variety of simple and commonly used controllers, among them velocity-feedback controllers and lead-lag compensators, are more than sufficient to perform such control. This is achieved by the judicious placement of sensors in the system and the acquisition of data from those locations with specific time delays. While it has been known for some time that collocated control (where the sensor and actuator are placed at the same location) leads to complete controllability of the system [6] with no spillover, similar results for noncollocated systems are rare [13]. In fact, it is known that noncollocation of sensors and actuators generally results in loss of controllability due to spillover effects.

Major differences from prior work are the following: (1) we show that *three* sensors are sufficient for preventing spillover under rather general boundary conditions for systems modeled by the one-dimensional wave equation; (2) the closed-loop transfer function is provided in explicit closed form through the use of Mathematica; and (3) we provide explicit expressions for the determination of the closed-loop poles and thus obtain simple expressions for upper bounds on the control gain so that stability is ensured.

In Section I we introduce some basic preliminaries about the distributed parameter system, and establish our notation. Section II deals with some key properties of the mechanical responses of such a system, which we then use in obtaining proper sensor placement locations and the correct time delays. The heuristics developed in this section are the key to the finite-dimensional control design provided in this paper. Section III deals with closed-loop feedback control and the associated Green's functions as well as the closed-loop transfer function for the distributed system. Section IV deals with stability issues and provides explicit bounds for the controller gain to ensure controllability. Section V presents some simulation results, and Section VI gives the conclusions. We provide three appendices in which several of the mathematical details are given.

I. SYSTEM MODEL

Consider a spatially distributed system subjected to a time varying force $f(x,t)$ described by

$$z_{tt} = c^2 z_{xx} + f(x,t), \tag{1}$$

where the space parameter x extends from 0 to L. The wave speed in the medium is denoted by c, and $f(x,t)$ is the force normalized with respect to the inertial mass per unit length of the medium. The subscripts t and x refer to differentiation with respect to time t and space x. This equation, though simplistic, governs the motion $z(x,t)$ of diverse systems such as the torsional vibrations of bars, the axial vibrations of rods, the horizontal motions of buildings, etc. We shall assume that the boundary conditions are given by

$$z_x(0,t) - h_1 z(0,t) = 0 \tag{2}$$

and

$$z_x(L,t) + h_2 z(L,t) = 0, \tag{3}$$

and that the initial conditions are $z_t(x,0) = z(x,0) = 0$.

The parameters h_1 and h_2 will be taken to be nonnegative. We shall assume throughout this paper that the boundary conditions are such that the operator is self-adjoint, and that its inverse is compact and positive definite. The eigenvalue problem associated with Equation (1) may then be obtained as

$$u_{xx} + \beta^2 u = 0, \qquad \beta^2 = \frac{\omega^2}{c^2} \tag{4}$$

with

$$u_x(0) - h_1 u(0) = 0 \tag{5}$$

and

$$u_x(L) + h_2 u(L) = 0. \tag{6}$$

The general solution of (4) is

$$u(x) = A\cos\beta x + B\sin\beta x = C\sin(\beta x + \phi), \tag{7}$$

where A and B are constants. Using (5) we obtain

$$u(x) = B\left(\frac{\beta}{h_1}\cos\beta x + \sin\beta x\right), \tag{8}$$

and using (6) we obtain the natural frequencies of vibration of the system from the roots of the equation

$$\cot\beta_n L = \frac{\beta_n^2 - h_1 h_2}{\beta_n(h_1 + h_2)}. \tag{9}$$

The roots β_n of Equation (9) provide the countably infinite set of eigenvalues of the system described by Equations (4), (5), and (6). We shall denote them by $\beta_1, \beta_2, \ldots, \beta_n, \ldots$. The corresponding eigenfunctions may be found as

$$u_n = \frac{\beta}{h_1}\cos\beta_n x + \sin\beta_n x, \tag{10}$$

or

$$u_n = \sin(\beta_n x + \phi_n) \tag{11}$$

where

$$\phi_n = \tan^{-1}\left(\frac{\beta_n}{h_1}\right). \tag{12}$$

Furthermore, there are no repeated eigenvalues, and the eigenfunctions are orthogonal to each other. It can also be shown that

$$\|u_n\|_2 = N_n = \int_0^L \sin^2(\beta_n x + \phi_n)\,dx,$$

$$= \frac{1}{2}\left[L + \frac{(\beta_n^2 + h_1 h_2)(h_1 + h_2)}{(\beta_n^2 + h_1^2)(\beta_n^2 + h_2^2)}\right]. \tag{13}$$

We note that the boundary conditions (5) and (6) refer to an elastically restrained system. We now make the following remarks.

REMARK 1.1. When $h_1 \to 0$, we have a free end at $x = 0$, and the phase angle ϕ_n, by Equation (12), is $\pi/2$, yielding $u_n = \cos\beta_n x$, with the characteristic equation given by

$$\tan\beta_n L = \frac{h_2}{\beta_n}.$$

REMARK 1.2. When $h_1 \to \infty$, the end $x = 0$ is fixed and $\phi_n = 0$. Thus $u_n = \sin\beta_n x$, and the characteristic equation becomes

$$\tan\beta_n L = \frac{-\beta_n}{h_2}.$$

REMARK 1.3. When $h_1, h_2 \to \infty$, we have a fixed-fixed system, the eigenfunction becomes $u_n = \sin\beta_n x$, $\phi_n = 0$, and the eigenvalues are $\beta_n = n\pi/L$, $n = 1, 2, \ldots$.

REMARK 1.4. When $h_1 \to \infty$, $h_2 \to 0$, we have a fixed-free system and the eigenfunctions are

$$u_n = \sin\beta_n x, \quad \beta_n = \frac{(2n-1)\pi}{2L}, \qquad n = 1, 2, \ldots.$$

REMARK 1.5. The roots of Equation (9) are real.

REMARK 1.6. The eigenfuctions of Equation (4) are always of the form

$$u_n = \sin(\beta_n x + \phi_n).$$

The boundary conditions affect the eigenvalues β_n, the phase angle ϕ_n, and $\|u_n\|_2$. We shall return to this later.

Using the eigenfunctions, which form a complete orthogonal set, we can now express the solution of Equation (1) subject to the conditions (2) and (3) as

$$z(x,t) = \sum_{n=1}^{\infty} a_n(t)u_n(x). \tag{14}$$

Taking Laplace transforms, we obtain

$$z(x,s) = \sum_{n=1}^{\infty} a_n(s)u_n(x). \tag{15}$$

Using (1), the orthogonality of $u_n(x)$, and (13), we obtain for each mode

$$a_n(s) = \frac{1}{N_n}\int_0^L \frac{u_n(x)f(x,s)\,dx}{s^2+\omega_n^2}. \tag{16}$$

The total response is then found using (14) as

$$z(x,s) = \int_0^L \left\{ \sum_1^{\infty} \frac{u_n(\xi)u_n(x)}{N_n(s^2+\omega_n^2)} \right\} f(\xi,s)\,d\xi. \tag{17}$$

The quantity in braces is the Green's function, and we will denote it by

$$g_0(x,\xi,s) = \sum_{n=1}^{n=\infty} \frac{u_n(x)u_n(\xi)}{N_n(s^2+\omega_n^2)} = \sum_{n=1}^{\infty} \frac{\sin(\beta_n x+\phi_n)\sin(\beta_n \xi+\phi_n)}{N_n(s^2+\omega_n^2)}, \tag{18}$$

so that

$$z(x,s) = \int_0^L g_0(x,\xi,s)f(\xi,s)\,d\xi. \tag{17a}$$

The open-loop transfer function $g_0(x,\xi,s)$ has an infinite number of poles at $s = \pm i\omega_n$. Using Remark 1.5, we see that these poles always lie along the imaginary axis.

II. A KEY PROPERTY OF MODAL RESPONSES

We now provide [14, 15] certain results which will be the key to obtaining noncollocated control designs for the system of Equation (1). In what follows we shall use our physical understanding of the way the mode shapes behave in the system characterized by Equation (1).

We begin by noting that the eigenfunction response (using separation of variables) of the system governed by Equation (1) looks like

$$u_n(x,t) = \sin(\beta_n x+\phi_n)\,e^{i\omega_n(t+\psi_n)}, \tag{19}$$

which can be expressed as

$$u_n(x,t) = \frac{e^{i(\beta_n x+\phi_n)} - e^{-i(\beta_n x+\phi_n)}}{2i} \times e^{ic\beta_n(t+\psi_n)}. \tag{20}$$

Furthermore, for any location $x_1 > x_2$ we have

$$u_n\left(x_1, t-\frac{x_2}{c}\right) - u_n\left(x_2, t-\frac{x_1}{c}\right)$$
$$= u_n(x_1-x_2,t) - e^{-i\beta_n(x_1-x_2-ct)}\sin\phi_n\, e^{i\omega_n\psi_n}, \tag{21}$$

and, similarly, for any location $x_a > x_3$ we get

$$u_n\left(x_a, t-\frac{x_3}{c}\right) - u_n\left(x_3, t-\frac{x_a}{c}\right)$$
$$= u_n(x_a-x_3,t) - e^{-i\beta_n(x_a-x_3-ct)}\sin\phi_n\, e^{i\omega_n\psi_n}. \tag{22}$$

The subscript a on x denotes, as we shall see in the next section, the actuator location. If we further choose the locations $x_a > x_3$ such that $x_1 - x_2 = x_a - x_3$ and subtract equation (22) from (21), we obtain

$$u_n\left(x_a, t-\frac{x_3}{c}\right) = u_n\left(x_1, t-\frac{x_2}{c}\right) + u_n\left(x_3, t-\frac{x_a}{c}\right) - u_n\left(x_2, t-\frac{x_1}{c}\right)$$
$$\forall n, \forall t. \tag{23}$$

Without loss of generality we can choose $x_a < x_1$ so that $x_3 < x_2$. Then

time-shifting equation (23) by x_3/c, we get

$$u_n(x_a,t) = u_n(x_1,t-T_1) + u_n(x_3,t-T_3) - u_n(x_2,t-T_2), \quad (24)$$

where

$$T_1 = \frac{x_2 - x_3}{c},$$

$$T_2 = \frac{x_1 - x_3}{c},$$

$$T_3 = \frac{x_a - x_3}{c}. \quad (25)$$

The time delays T_1, T_2, T_3 are all positive, and thus we have been able to obtain a perfect "predictor" for the nth mode response at location x_a at time t by looking at the nth-mode response at locations x_1, x_2, and x_3 at times $t-T_1$, $t-T_2$, and $t-T_3$ respectively. To predict the response of the nth mode ($n = 1,2,\ldots$) at location x_a we therefore need, in general, *three sensors*. We note that $x_1 - x_2 = x_a - x_3$. The location of x_a relative to x_2 is left open for now. Two possible configurations could arise: (1) $x_3 < x_a < x_2 < x_1$ and (2) $x_3 < x_2 < x_a < x_1$. For both these conditions, the relations (24) and (25) are valid. In Section V we shall see however that there is some difference in these two configurations in that they lead to different bounds on the controller gains to ensure stability.

REMARK II.1. The time delays T_1, T_2, T_3 in Equations (24) and (25) do not involve the mode number, and therefore the same three locations and the same three delays will provide predictions for all modes.

REMARK II.2a. When $\phi_n = 0$ (see Remarks I.2, I.3 and I.4), Equation (21) yields, for $x_1 > x_a$ [12]

$$u_n(x_a,t) = u_n\left(x_1, t - \frac{x_2}{c}\right) - u_n\left(x_1 - x_a, t - \frac{x_1}{c}\right) \qquad \forall n, \forall t. \quad (23a)$$

Thus to predict the nth mode response at time t at location x_a we need sensors at locations x_1 and $x_2 = x_1 - x_a$. Data on the nth mode obtained at times $t - x_2/c$ and $t - x_1/c$ respectively yield "perfect predictions" of the nth mode response at location x_a at time t. Since the time delays are independent of the mode number, these statements are true for any mode.

REMARK II.2b. Furthermore, for the fixed-fixed system (see Remark I.3), we obtain

$$u_n(x_a,t) = -u_n\left(L - x_a, t - \frac{L}{c}\right) \qquad \forall n, \forall t. \quad (23b)$$

Thus one sensor located at $L - x_a$ will predict $u_n(x_a,t)$, $n = 1,2,\ldots$. This can also be obtained as a special case of the bandsaw problem discussed in [13] when the bandsaw speed is set to zero.

REMARK II.3. In Remark I.6 we observed that the eigenfunctions $\sin(\beta_n x + \phi_n)$, $n = 1,2,\ldots$, are the most general for the problem (4). Thus Equation (24) with (25) is valid for arbitrary boundary conditions.

REMARK II.4. One way of determining $u_n(x_a,t)$ is to place a sensor at $x = x_a$. This would amount to collocation of the sensor and the actuator. If one does not place a sensor at x_a, then $u_n(x_a,t)$ can be obtained by using Equations (24) and (25), but in general three sensors are required. We then observe that there is a cost associated with noncollocation, i.e., the use of two additional sensors to obtain the nth mode response at location x_a. This cost can be reduced to one additional sensor in situations for which $\phi_n = 0$, i.e., when one of the ends is fixed (as shown in Remark II.2a). For the fixed-fixed situation (as shown in Remark II.2b), there is no cost associated with noncollocation.

REMARK II.5. In the same manner as in Equation (24), we can show that

$$u_n(x_a) = u_n(x_1)e^{\pm i\omega_n T_1} + u_n(x_3)e^{\pm i\omega_n T_3} - u_n(x_2)e^{\pm i\omega_n T_2} \qquad \forall n. \quad (26)$$

This result is valid for all modes n. It is physically indicative of the fact that the response of the nth mode at a location x_a and time t can be precisely

predicted by the response at three locations x_1, x_2, x_3 with appropriate time delays T_1, T_2, and T_3. We shall use this important result later in Section IV and in several proofs presented in the appendices.

III. CLOSED-LOOP CONTROL

Having realized that we can obtain a prediction of $u_n(x_a, t)$ by using at most three sensors at locations x_1, x_2, and x_3 as described in the previous section, we can now design a feedback controller for the distributed system of Equation (1), where the location x_a of the actuator is chosen so that (1) it does not lie on any node of any mode of the system, and (2) $x_1 - x_2 = x_a - x_3$.

Figure 1 shows the control design. The sensors, which are located at x_1, x_2, x_3, are polled, as shown in the figure, at time delays of T_1, T_2, and T_3

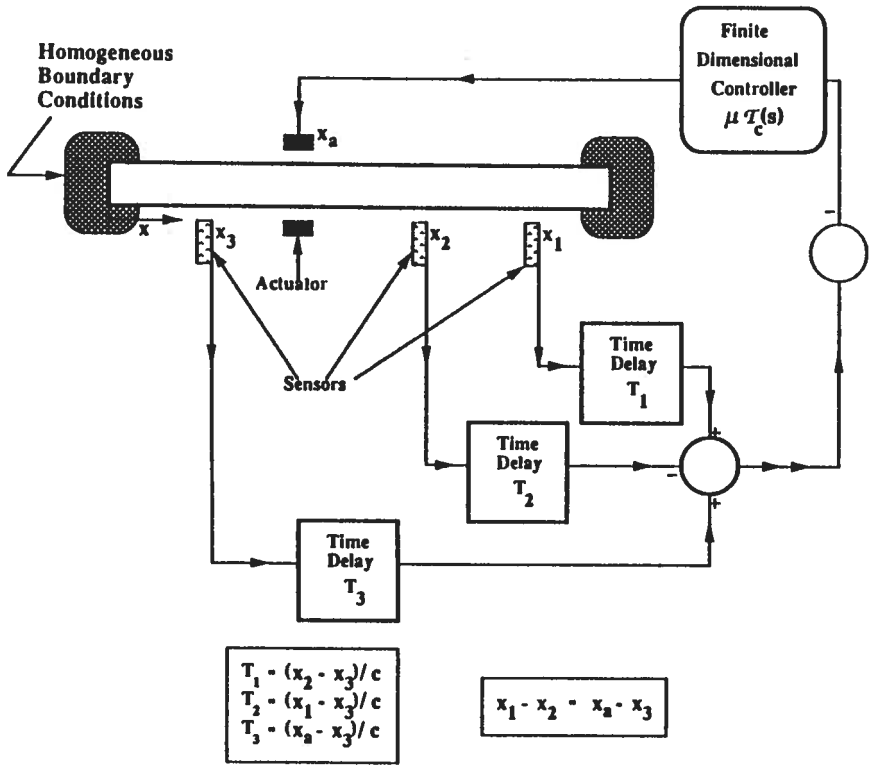

FIG. 1. Noncollocated time-delayed control design showing three sensors at locations x_1, x_2, and x_3, and an actuator at location x_a. The arrangement corresponds to configuration C1.

respectively. The outputs from the sensors located at x_1 and x_3 are added together, those from x_2 are subtracted, and the combined signal is multiplied by minus one and then fed to a finite-dimensional controller. The controller has a transfer function $\mu\mathcal{T}_c(s) := \mu K(s)/P(s)$, where μ is the controller gain. We shall assume, in what follows, that $K(i\omega) \neq 0$ for all ω.

Our physical understanding of the problem is as follows. The placement of three sensors at locations x_1, x_2, and x_3 (as described in Figure 1) becomes tantamount [see Equation (24)] to placing *one* sensor at the actuator location, x_a itself—and hence an effective collocation of the sensor with the actuator —provided we use the properly time-delayed data from these three sensors appropriately. One would therefore heuristically expect that results on controllability that apply to collocated sensor and actuator designs would also apply to our noncollocated sensor and actuator design. More specifically, since one can always design a stable closed-loop control using collocated sensors and actuators, this result should then also apply to our noncollocated system of Figure 1.

Using Equation (17a) and letting $f(\xi, s) = f_d(\xi, s) - f_c(u, s)$, where f_c represents the feedback control force and f_d the disturbance, we obtain

$$z(x,s) = \int_0^L g_0(x,\xi,s)\left[f_d(\xi,s) - f_c(\xi,s)\right] d\xi. \tag{27}$$

Using an actuator at location x_a, we obtain (see Figure 1)

$$f_c(\xi,s) = \mu\mathcal{T}_c(s)\left[z(x_1,s)e^{-sT_1} - z(x_2,s)e^{-sT_2} + z(x_3,s)e^{-sT_3}\right] \times \delta(\xi - x_a). \tag{28}$$

Equation (27) then becomes

$$z(x,s) = \int_0^L g_0(x,\xi,s) f_d(\xi,s)\, ds - g_0(x,x_a,s)\mu\mathcal{T}_c(s)\left[z(x_1,s)e^{-sT_1} - z(x_2,s)e^{-sT_2} + z(x_3,s)e^{-sT_3}\right]. \tag{29}$$

Denoting

$$\alpha(x,x_a,s)=\mu\mathscr{T}_c(s)g_0(x,x_a,s), \tag{30}$$

$$F_d(x,s)=\int_0^L g_0(x,\xi,s)f_d(\xi,s)\,d\xi, \tag{31}$$

$$\mathscr{F}(s)=\begin{bmatrix}F_d(x_1,s) & F_d(x_2,s) & F_d(x_3,s)\end{bmatrix}^T, \tag{32}$$

$$\mathbf{G}_0(\xi,s)=\begin{bmatrix}g_0(x_1,\xi,s) & g_0(x_2,\xi,s) & g_0(x_3,\xi,s)\end{bmatrix}^T, \tag{33}$$

$$\mathbf{d}=\begin{bmatrix}e^{-sT_1} & -e^{-sT_2} & e^{-sT_3}\end{bmatrix}^T, \tag{34}$$

$$\mathscr{Z}(s)=\begin{bmatrix}z(x_1,s) & z(x_2,s) & z(x_3,s)\end{bmatrix}^T, \tag{35}$$

$$J(\xi)=\mathbf{d}^T(s)\mathbf{G}_0(\xi,s), \tag{36}$$

Equation (29) can be written as

$$z(x,s)=F(x,s)-\alpha(x,x_a,s)\mathbf{d}^Tz(s). \tag{37}$$

Letting $x=x_1$, x_2, and x_3 in (37) yields the set of simultaneous equations

$$A\mathscr{Z}=\mathscr{F}, \tag{38}$$

where

$$A=\begin{bmatrix}1+\alpha(x_1,x_a,s)e^{-sT_1} & -\alpha(x_1,x_a,s)e^{-sT_2} & \alpha(x_1,x_a,s)e^{-sT_3}\\ \alpha(x_2,x_a,s)e^{-sT_1} & 1-\alpha(x_2,x_a,s)e^{-sT_2} & \alpha(x_2,x_a,s)e^{-sT_3}\\ \alpha(x_3,x_a,s)e^{-sT_1} & -\alpha(x_3,x_a,s)e^{-sT_2} & 1+\alpha(x_3,x_a,s)e^{-sT_3}\end{bmatrix}. \tag{39}$$

This yields

$$\mathscr{Z}=A^{-1}\mathscr{F}, \tag{40}$$

so that (37) becomes

$$z(x,s)=F(x,s)-\alpha(x,x_a,s)\mathbf{d}^TA^{-1}\mathscr{F}. \tag{41}$$

We next present two properties of the matrix A.

REMARK III.1.

$$\begin{aligned}\det A&=1+\alpha(x_1,x_a,s)e^{-sT_1}-\alpha(x_2,x_a,s)e^{-sT_2}+\alpha(x_3,x_a,s)e^{-sT_3}\\&=1+\mu\mathscr{T}_c(s)\mathbf{d}^T(s)\mathbf{G}_0(x_a,s)=1+\mu\mathscr{T}_c(s)J(x_a,s).\end{aligned} \tag{42}$$

The first result can be directly verified. The others are notationally convenient.

REMARK III.2.

$$\mathbf{d}^TA^{-1}=\frac{1}{\det A}\mathbf{d}^T. \tag{43}$$

The result can be directly calculated.

We then obtain for the closed-loop response

$$\begin{aligned}z(x,s)=\frac{1}{\det A}\int_0^L&\left[(\det A)\,g_0(x,\xi,s)-\alpha(x,x_a,s)\mathbf{d}^T\mathbf{G}_0(\xi,s)\right]\\&\times f_d(\xi,s)\,d\xi.\end{aligned} \tag{44}$$

This yields the closed-loop transfer function

$$G_{cl}(x,\xi,s)=\frac{(\det A)\,g_0(x,\xi,s)-\alpha(x,x_a,s)\mathbf{d}^T\mathbf{G}_0(\xi,s)}{\det A}. \tag{45}$$

The closed-loop poles (see Appendix 1) then lie at the roots of

$$\begin{aligned}\det A=1+\mu\mathscr{T}_c(s)\big[&g_0(x_1,x_a,s)e^{-sT_1}+g_0(x_3,x_a,s)e^{-sT_3}\\&-g_0(x_2,x_a,s)e^{-sT_2}\big]=0.\end{aligned} \tag{46}$$

The denominator of Equation (45) contains one term which involves the open-loop poles of the system. However, on careful examination we find that the closed-loop transfer function cannot share poles with the open-loop transfer function for any positive value of μ. This is shown in Appendix 1. Thus for positive values of μ, the roots of Equation (46) provide all the closed-loop poles.

Of primary interest to us is the ability to control all modes of vibration, thereby eliminating any spillover of uncontrollable modes. To do this we next look at the stability of our feedback controller.

IV. STABILITY AND CONTROLLER DESIGN

1. *Stability for Small Gains* μ

To study the stability of the control design, we shall use the following stability criterion. Noting that the open-loop poles occur at the frequencies $s_k = \pm i\omega_k$ where ω_k is real, the root locus $s_k(\mu)$ of the kth closed-loop pole, which starts for $\mu = 0$ at ω_k on the imaginary axis, will move to the left half s-plane if [13]

$$\operatorname{Re}\left\{\frac{ds_k}{d\mu}\right\}_{\mu=0+} < 0 \qquad \forall k. \tag{47}$$

If this condition is satisfied, then in the close vicinity of $\mu = 0$, all the poles will have negative real parts and will therefore be stable. Using the expansion (18) for $g_0(x_i, x_a, s)$ in (46), we get the following condition for the closed-loop poles:

$$1 + \mu\mathscr{T}_c(s)\left[\sum_{n=1}^{\infty} \frac{u_n(x_a)}{N_n(s^2+\omega_n^2)}\{u_n(x_1)e^{-sT_1} + u_n(x_3)e^{-sT_3} - u_n(x_2)e^{-sT_2}\}\right] = 0. \tag{48}$$

Noting that at $\mu = 0$ the zeros of (45) are the open loop poles $s = s_k = \pm i\omega_k$, $k = 1,2,\ldots,\infty$, and using Remark II.5, we require by Equation (47) (see Appendix 2) that for $k = 1,2,\ldots,\infty$,

$$\operatorname{Re}\left\{\frac{ds_k}{d\mu}\bigg|_{\mu=0+}\right\} = -\frac{u_k^2(x_a)}{2N_k}\operatorname{Re}\left\{\lim_{s\to\pm i\omega_k}\left[\frac{\mathscr{T}_c(s)}{s}\right]\right\} < 0. \tag{49}$$

Using Equation (49), we can now design controllers which satisfy Equation (49) and are therefore stable. Taking the controller's transfer function as

$$\mathscr{T}_c(i\omega) := \frac{K(i\omega)}{P(i\omega)} = a(\omega) + ib(\omega), \tag{50}$$

where $K(i\omega)$ and $P(i\omega)$ can be taken to be polynomials, the condition (49) requires that at *each* open-loop pole,

$$\lim_{\omega\to\pm\omega_k}\frac{b(\omega)}{\omega} > 0, \qquad k = 1,2,\ldots,\infty, \tag{51}$$

since $N_k = \|u_n\|_2 > 0$, and x_a is not at any node of any mode.

If we choose $b(\omega)$ to be a continuous function, we then need it to be an odd function of ω, with $b(0) = 0$, $b(\omega) > 0$, $\omega \in (0,\infty)$. *Throughout this paper we will assume that* $b(\omega)$ *of the controller's transfer function has this property.* We shall refer to this property as P1.

Examples of a few simple finite-dimensional controllers that satisfy P1 are:

(1) a velocity feedback controller with

$$\mathscr{T}_c(i\omega) = i\omega, \tag{52}$$

(2) a lag-lead compensator (with more lead than lag),

$$\mathscr{T}_c(i\omega) = \frac{1+i\omega\tau_1}{1+i\omega\tau_2}, \qquad \tau_1 > \tau_2 > 0. \tag{53}$$

We have so far proved stability when the controller gain μ is positive, though vanishingly small.

We note in passing that the stability result obtained in Equation (51) (and property P1) can also be derived using passivity theory (see, for example, [8]).

REMARK IV.1. While we have dealt in this paper with the general boundary-condition situation, the results on the stability of the closed-loop system in the case of two sensors (when $\phi_n = 0$, see Remark II.2a) and in the case of one sensor (for the fixed-fixed system, see Remark II.2b) follow *mutatis mutandis*. For each situation the modal response at (x_a, t) is obtained

from responses at other locations at previous times. In each case the closed-loop transfer function is stable, and controllers such as the two stated above in Equations (52)–(53) will bring about stabilization of the system [see Remark II.2, Equations (22) and (23)] for vanishingly small gains. We note in passing that for the "fixed-fixed" system (see Remark I.3 and Remark II.2b) a phase shift of 180 degrees needs to be added to the controller, as seen from Equation (23b).

REMARK IV.2. The argument in this section is valid provided $u_k(x_a) \neq 0$, i.e., x_a is not located at a node of any mode of the system. Since the nodes of the modes form only a countable infinity, this is, at least theoretically, clearly possible

REMARK IV.3. We note that for the system to be stabilized using vanishingly small gains, the condition (51) need be satisfied only at the open-loop poles of the system.

REMARK IV.4. The simple controllers used in equations (52) and (53) have imaginary parts greater than zero for $\omega > 0$. We note that for $\omega = 0$, their imaginary parts are zero; yet the limit indicated in Equation (51) exists for each of them, and the inequality in (51) is satisfied. Thus even for systems that have rigid-body modes (e.g., when h_1 and h_2 are both zero so that $\omega_1 = 0$), the condition (51) is not violated by the simple controllers described above.

We shall come back to this remark in the next subsection, when we shall provide explicit values of the bounds on μ for stabilization of the closed-loop system.

2. *The Development of an Upper Bound $\mu^{\max}$ for the Controller Gain*

We denote by $\mu^{\max}$ the upper bound on μ up to which the closed-loop control described in this paper is stable. In this subsection we show that one can actually provide explicit expressions for a parameter M, $M > 0$, such that $\mu^{\max} \geq M$ for the closed-loop, time-delayed, noncollocated system to be stable when the controller's transfer function $\mathscr{T}_c$ satisfies property P1.

As mentioned in Section II, we will now distinguish between the two different sensor and actuator placement configurations: (1) configuration C1, when $x_3 < x_a < x_2 < x_1$, and (2) configuration C2, when $x_3 < x_2 < x_a < x_1$. The development of an upper bound in terms of the locations of the sensors

and the actuators can be developed as follows. (For the mathematical details refer to Appendix 3.)

(1) We begin with the Green's function of the form shown in Equation (A.10) (see Appendix 3) which is valid for the problem stated in Equation (1) with arbitrary boundary conditions.

(2) We show (Appendix 3, Lemmas 5 and 6) that the closed-loop transfer-function poles are the zeros of the equations

$$1 + \mu \mathscr{T}_c(s)\left[g_0(x_a, x_a, s) - \frac{e^{-\bar{\beta}(x_a - x_3)}}{c^2\bar{\beta}} \sinh \bar{\beta}(x_a - x_3)\right] = 0 \qquad \text{for C1} \tag{54}$$

and

$$1 + \mu \mathscr{T}_c(s)\left[g_0(x_a, x_a, s) - \frac{e^{-\bar{\beta}(x_2 - x_3)}}{c^2\bar{\beta}} \sinh \bar{\beta}(x_2 - x_3)\right] = 0 \qquad \text{for C2,} \tag{55}$$

where $s^2 = c^2\bar{\beta}^2$.

(3) We have shown stability small positive gains when the controller's transfer function $\mathscr{T}_c(i\omega) := a(\omega) + ib(\omega)$ is such that property P1 is satisfied. In that case the root loci of the closed-loop poles, for infinitesimal gains, will move towards the left half s-plane. We observe that before the root locus of any pole bent back and moved into the right half s-plane it would have to cross the imaginary axis.

(4) We show (in Appendix 3, Result A.3) that one of the conditions for this crossing to occur at $s = \pm i\eta$ is

$$\sin^2\left\{\frac{\eta(x_a - x_3)}{c}\right\} = \frac{c}{\mu}\left\{\frac{\eta b(\eta)}{a^2(\eta) + b^2(\eta)}\right\} \qquad \text{for C1} \tag{56a}$$

and

$$\sin^2\left\{\frac{\eta(x_2 - x_3)}{c}\right\} = \frac{c}{\mu}\left\{\frac{\eta b(\eta)}{a^2(\eta) + b^2(\eta)}\right\} \qquad \text{for C2.} \tag{56b}$$

These relations result from setting the imaginary and real parts of Equations (54) and (55) to zero for $s = \pm i\eta$.

Consider the class of controllers for which $a(0) > 0$. Many commonly used controllers fall in this category [e.g., Equation (53)]. Then Equation (56) is satisfied when $\eta = 0$. This corresponds to a value of μ given by (we assume that the appropriate limits exist, i.e., no rigid-body modes)

$$\frac{1}{\mu \mathscr{T}_c(0)} = -\left[\lim_{s\to 0} g_0(x_a, x_a, s) - \frac{x_a - x_3}{c^2}\right] \qquad \text{for C1} \qquad (57a)$$

and

$$\frac{1}{\mu \mathscr{T}_c(0)} = -\left[\lim_{s\to 0} g_0(x_a, x_a, s) - \frac{x_2 - x_3}{c^2}\right] \qquad \text{for C2.} \qquad (57b)$$

The Green's function $g(x_a, x_a, 0)$ can be interpreted as the response of the system at location x_a to a static load applied at x_a, and is therefore always positive. Thus as long as

$$\lim_{s\to 0} g_0(x_a, x_a, s) > \frac{x_a - x_3}{c^2} \qquad \text{for C1} \qquad (58a)$$

and,

$$\lim_{s\to 0} g_0(x_a, x_a, s) > \frac{x_2 - x_3}{c^2} \qquad \text{for C2,} \qquad (58b)$$

the values of μ will be negative and therefore will be irrelevant to obtaining a bound on it.

The left-hand side of Equation (56) has a maximum value of unity when

$$\eta_k^* = \pm \frac{(2k-1)\pi c}{2(x_a - x_3)}, \quad k = 1, 2, \ldots, \qquad \text{for configuration C1} \quad (59a)$$

and

$$\eta_k^* = \pm \frac{(2k-1)\pi c}{2(x_2 - x_3)}, \quad k = 1, 2, \ldots, \qquad \text{for configuration C2.} \quad (59b)$$

We can then ensure that Equation (56) will *not* be satisfied by choosing a μ

such that

$$\frac{c}{\mu}\left[\frac{\eta b(\eta)}{a^2(\eta) + b^2(\eta)}\right] > \sin^2\left\{\frac{\pm \eta y}{c}\right\} \qquad \text{for all } \eta, \qquad (60)$$

where y equals $x_a - x_3$ for configuration C1, and $x_2 - x_3$ for configuration C2. Furthermore, when the fraction in brackets on the left-hand side in equation (60) is a monotone increasing function of η, and the condition (58) is satisfied, a bound M for $\mu^{\max}$ can often be found by ensuring that the left-hand side is greater than unity at η_1^*. This yields (see Example 2, Section V)

$$\mu^{\max} \geq M = \left\{\frac{\eta_1^* b(\eta_1^*)}{a^2(\eta_1^*) + b^2(\eta_1^*)}\right\} \cdot c, \qquad (61)$$

where η_1^* is as defined in equation (59) for the two configurations C1 and C2. Note that the conditions (58) and (60) ensure that the root locus does not cross the imaginary axis. As indicated in Equation (61), the upper bound on μ for stability could, in general, be greater than M; for, even when $\mu > M$, the root locus may still *not* cross the imaginary axis. We have thus obtained a lower bound on $\mu^{\max}$. Stability is ensured for $0 < \mu < M \leq \mu^{\max}$. In the next section we show some numerical examples where the value of M obtained from Equation (61) is not too far from $\mu^{\max}$.

We note from Equation (61) that the value of M, when Equation (58) is satisfied, is dependent only on (1) the nature of the controller's transfer function, (2) the wave speed c in the medium, and (3) the separation distance $x_a - x_3$ for C1 or $x_2 - x_3$ for C2.

REMARK IV.5. When we use velocity feedback [$a(i\omega) = 0$, $b(i\omega) = \omega$ for all ω], the closed-loop control is stable for all $0 < \mu < c$, i.e., $M = c$.

We observe that the right-hand side of Equation (56) is now a constant whose value is c/μ. Thus $\eta = 0$ does not satisfy Equation (56). Furthermore, this equation cannot be satisfied as long as $\mu < c$; hence the result.

REMARK IV.6. The exact upper bound for μ in the case of velocity feedback can be obtained as a solution of the equation

$$1 + \mu \mathscr{T}_c(\bar{\beta}^* c)\left[g_0(x_a, x_a, s) - \frac{e^{-\bar{\beta}^*(x_a - x_3)}}{c^2 \bar{\beta}^*} \sinh \bar{\beta}^*(x_a - x_3)\right] = 0 \qquad \text{for C1}$$

(62a)

and

$$1+\mu\mathscr{T}_c(\bar{\beta}^* c)\left[g_0(x_a,x_a,s)-\frac{e^{-\bar{\beta}^*(x_2-x_3)}}{c^2\bar{\beta}^*}\sinh\bar{\beta}^*(x_2-x_3)\right]=0 \qquad \text{for C2,} \tag{62b}$$

where

$$\bar{\beta}_n^* = \pm\frac{i}{x_a-x_3}\left[n\pi \pm \sin^{-1}\left\{\sqrt{\frac{c}{\mu}}\right\}\right] \qquad \text{for C1} \tag{62c}$$

and

$$\bar{\beta}_n^* = \pm\frac{i}{x_2-x_3}\left[n\pi \pm \sin^{-1}\left\{\sqrt{\frac{c}{\mu}}\right\}\right] \qquad \text{for C2,} \tag{62d}$$

where $n = 0,1,2,3,\ldots$. This follows from Equation (56) and the observation in the previous remark. The smallest positive root, for any given $\mathscr{T}_c$, yields $\mu^{\max}$. We will show some numerical examples in the next section where the bound $M = c$ is shown to be adequate.

REMARK IV.7. The value of $\lim_{s\to 0} g_0(x_a,x_a,s)$ for the problem (1)–(3) is given in Lemma 10 of Appendix 3.

For the situations dealt with in Remarks I.1–I.4, we provide the following specific results:

(1) As $h_1 \to 0$,

$$\lim_{s\to 0}\{g_0(x_a,x_a,s)\} = \frac{1+h_2(L-x_a)}{h_2c^2}.$$

(2) As $h_1 \to \infty$,

$$\lim_{s\to 0}\{g_0(x_a,x_a,s)\} = \frac{x_a}{c^2} - \frac{x_a^2h_2}{(1+h_2L)c^2}.$$

(3) As $h_1 \to \infty$, $h_2 \to \infty$,

$$\lim_{s\to 0}\{g_0(x_a,x_a,s)\} = \frac{x_a}{c^2} - \frac{x_a^2}{Lc^2}.$$

(4) As $h_1 \to \infty$, $h_2 \to 0$,

$$\lim_{s\to 0}\{g_0(x_a,x_a,s)\} = \frac{x_a}{c^2}.$$

These results follow directly from Lemma 10, Appendix 3.

Note that when both h_1 and h_2 are both zero, the Green's function is unbounded; this is because we then have a rigid-body mode in the open-loop system whose natural frequency is zero. Furthermore, when h_1 and h_2 tend to infinity (for the fixed-fixed system), the condition (58a) requires that x_a/L be less than x_3/x_a; when h_1 tends to infinity and h_2 tends to zero (for the fixed-free system), the condition (58a) is always satisfied.

REMARK IV.8. If we *collocate* the sensor and the actuator, i.e., use one sensor and place it at the actuator location x_a, then the system described by Equation (1) can be stabilized by any controller whose transfer function $\mathscr{T}_c$ satisfies property P1 and for which $a(0) > 0$. We show here why this is true.

A collocated actuator-and-sensor pair become a special case of the control $f_c(\xi,s)$ described in Equation (28) when $x_1 = x_2 = x_3 = x_a$ and $T_1 = T_2 = T_3 = 0$. Results obtained earlier can therefore be particularized by making these substitutions in the expressions. In particular, the closed-loop transfer-function poles for collocation of sensors and actuators can be obtained from Equation (46) by setting $x_1 = x_2 = x_3 = x_a$ and $T_i = 0$, $i = 1,2,3$. The matrix A [see Equation (29)] now reduces to a scalar. Denoting this scalar by $A^{(\mathrm{col})}$ for the collocated case, we obtain, using Equations (46) and (18), the closed-loop poles from the following condition:

$$\det A^{(\mathrm{col})} = 1+\mu\mathscr{T}_c(s)\,g_0(x_a,x_a,s) = 1+\mu\mathscr{T}_c(s)\sum_{n=1}^{n=\infty}\frac{u_n^2(x_a)}{N_n(s^2+\omega_n^2)} = 0. \tag{63}$$

The derivative, $ds_k/d\mu|_{\mu=0+}$, can be obtained as before (see Appendix 2), and is given again by the expression in Equation (50). [This can also be seen by directly making the necessary substitutions in Equation (A.8) of Appendix 2.] The fact that this expression is the same as for the noncollocated situation indicates that the poles begin to move for the collocated case in exactly the same way as those for our dislocated control design with proper time delays; this points out that in some sense, for vanishingly small gains, the dislocation when done properly is tantamount to a collocation. Thus as long as the transfer function of the controller satisfies property P1, the root loci of all the poles s_k will move to the left half of the s-plane for infinitesimally positive values of μ.

It can be shown, as in Appendix 1, that the closed-loop poles for $\mu > 0$ cannot be coincident with the open-loop poles. Thus, for the root locus of any pole to move into the positive half s-plane, we would require that it cut the imaginary axis at some $s = \pm i\eta$. Hence, for the closed-loop control to lose stability for some value of μ, Equation (55) must be satisfied for $s = \pm i\eta$.

This requires, for $\mu > 0$, that

$$\frac{1}{\mu} + a(i\eta)g_0(x_a, x_a, i\eta) + ib(i\eta)g_0(x_a, x_a, i\eta) = 0. \tag{64}$$

If $g(x_a, x_a, i\eta) = 0$, Equation (64) cannot be satisfied [we assume that $b(i\eta)$ is bounded]. Let $g(x_a, x_a, i\eta) \neq 0$; since $g(x_a, x_a, i\eta)$, $a(i\eta)$, and $b(i\eta)$ are all real numbers, this requires the imaginary part of Equation (64) to be zero. For a controller that satisfies property P1 and for which $b(i\eta)$ is continuous and positive for $\eta \in (0, \infty)$, this is clearly impossible unless $\eta = 0$. Setting $\eta = 0$ in Equation (64), we find that the closed-loop poles must satisfy [we assume that $g_0(x_a, x_a, 0)$ exists, i.e., no rigid-body motion]

$$\frac{1}{\mu} + a(0)g_0(x_a, x_a, 0) = 0, \tag{65}$$

which is impossible for any positive value of μ provided that $a(0) \geq 0$, since $g(x_a, x_a, 0)$ is always positive. Hence collocation of the sensor and the actuator will cause the system to be stabilized for all controller gains, when the controllers satisfy property P1 and have $a(0) \geq 0$, e.g., for the controllers listed in equations (52)–(53). A weaker form of this result was provided by Balas [6] when he looked at velocity-feedback controllers.

Remark IV.9. When the sensor and actuator are dislocated and the time delay is zero, the system characterized by Equation (1) cannot be stabilized. Let us say that the sensor is located at x_1. This becomes again a special case of the control $f_c(\xi, s)$ described in Equation (28) when $x_1 = x_2 = x_3 \neq x_a$ and $T_1 = T_2 = T_3 = 0$. The matrix A is again a scalar, which we call $A^{(\text{ncol})}$ to denote noncollocation. Making the necessary substitutions in Equation (46) and using Equation (18), we obtain

$$\det A^{(\text{ncol})} = 1 + \mu\mathscr{T}_c(s)g_0(x_1, x_a, s) = 1 + \mu\mathscr{T}_c(s)\sum_{n=1}^{n=\infty}\frac{u_n(x_1)u_n(x_a)}{N_n(s^2 + \omega_n^2)} = 0. \tag{66}$$

The derivative $ds_k/d\mu|_{\mu=0+}$ at the open loop pole $s_k = \pm i\omega_k$ then becomes

$$\left.\frac{ds_K}{d\mu}\right|_{\mu=0+} = -\frac{u_k(x_1)u_k(x_a)}{2N_K}\lim_{\omega\to\pm\omega_k}\frac{\mathscr{T}_c(\pm i\omega)}{\pm i\omega}, \tag{67}$$

whose real part cannot be guaranteed to be negative for all k, using a finite-dimensional controller. Hence dislocated control will not be able to stabilize our neutrally stable system using simple finite-dimensional controllers.

V. SIMULATION RESULTS

We now show some simulation examples of the control design that we have discussed in this paper.

Example 1 (Velocity-feedback control).

(a) We consider the system described by Equations (1)–(3) with the following parameters (assumed to be chosen in consistent units):

$$c = 2, \quad L = 1, \quad h_1 = 5000, \quad h_2 = 0.01,$$
$$x_a - x_3 = 0.34567892, \quad x_a = 0.47654321. \tag{S1}$$

The transfer function of the controller is given by $\mathscr{T}_c(i\omega) = i\omega$. We will use

TABLE I

Mode number	β_l
1	1.577
2	4.713
3	7.854
4	10.994
5	14.135
6	17.276
7	20.417
8	23.558
9	26.699
10	29.839

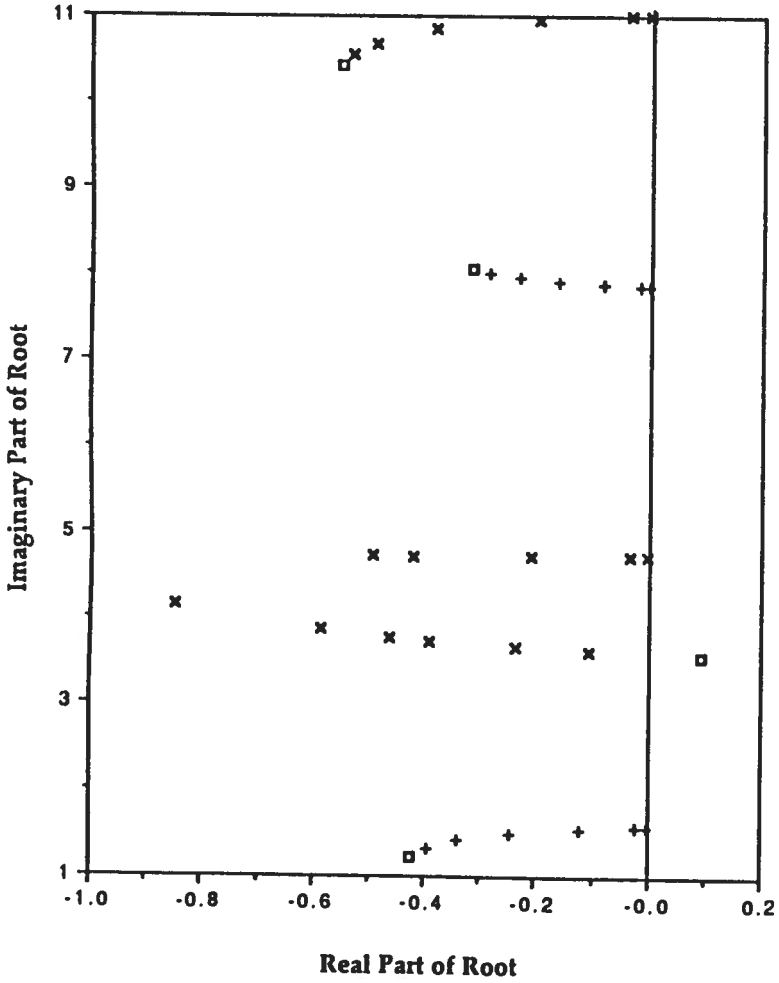

FIG. 2a. Velocity-feedback control for cantilever bar: the lowest four closed-loop poles, showing $\bar{\beta}$ for different values of μ. Pluses and crosses indicate roots for $0 < \mu < M$. Open squares indicate roots for $\mu > M$. The system is stable for $0 < \mu < M$.

configuration C1. The system is an approximation to a fixed-free system. The first ten frequencies $\beta_i = \omega_i / c$ are shown in Table 1. By Remark IV.6, $M = c = 2$, and we are assured stability as long as $0 < \mu < 2$. The root loci are shown in Figures 2a and 2b in the upper half s-plane for the first ten frequencies, using Equation (54). The roots $\bar{\beta}$ for different values of μ (typically $\mu = 0.01, 0.1, 0.5, 1, 1.5, 2$, and 2.5) are shown. The locations of the

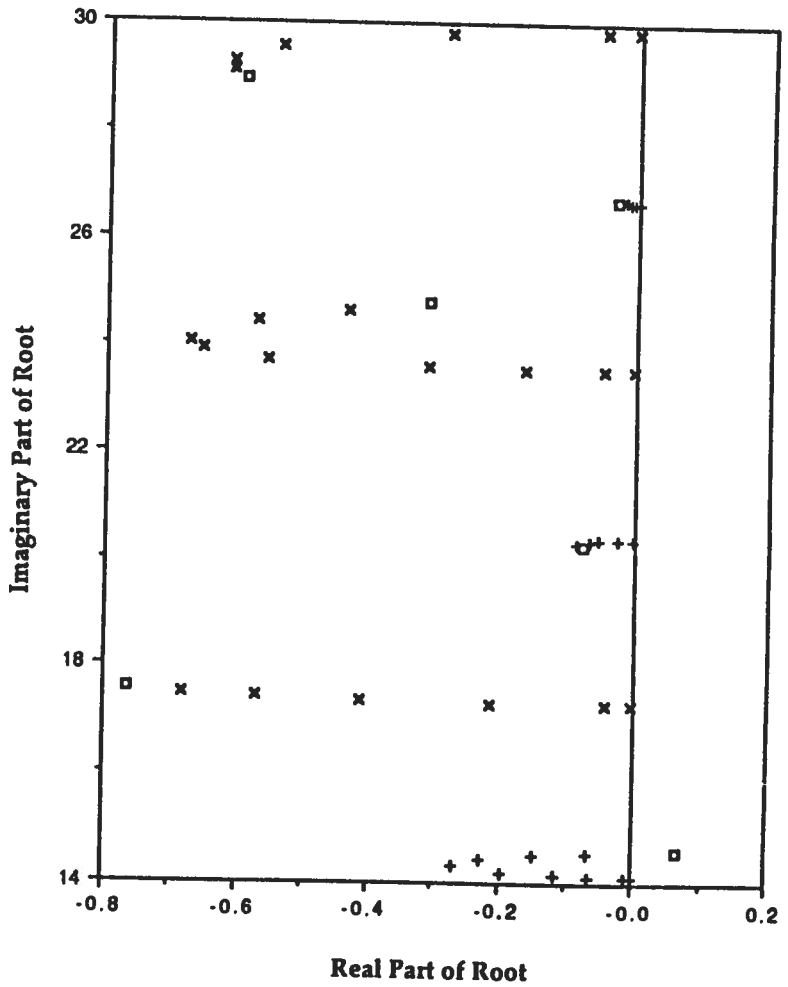

FIG. 2b. Velocity-feedback control for cantilever bar: the next six closed-loop poles, showing $\bar{\beta}$ for different values of μ. Pluses and crosses indicate roots for $0 < \mu < M$. Open squares indicate roots for $\mu > M$. The system is stable for $0 < \mu < M$.

roots for all values of $0 < \mu < M$ are indicated by crosses or pluses. The open squares show the roots for $\mu > M$. We observe that the closed-loop poles begin for $\mu = 0.01$ near the open-loop poles which lie on the imaginary axis. The root loci of the poles corresponding to the second and fifth modes are seen to curve around and move into the right half s-plane when $\mu = 2.5$. For $0 < \mu < M$, all the closed-loop poles lie in the left half s-plane, as expected.

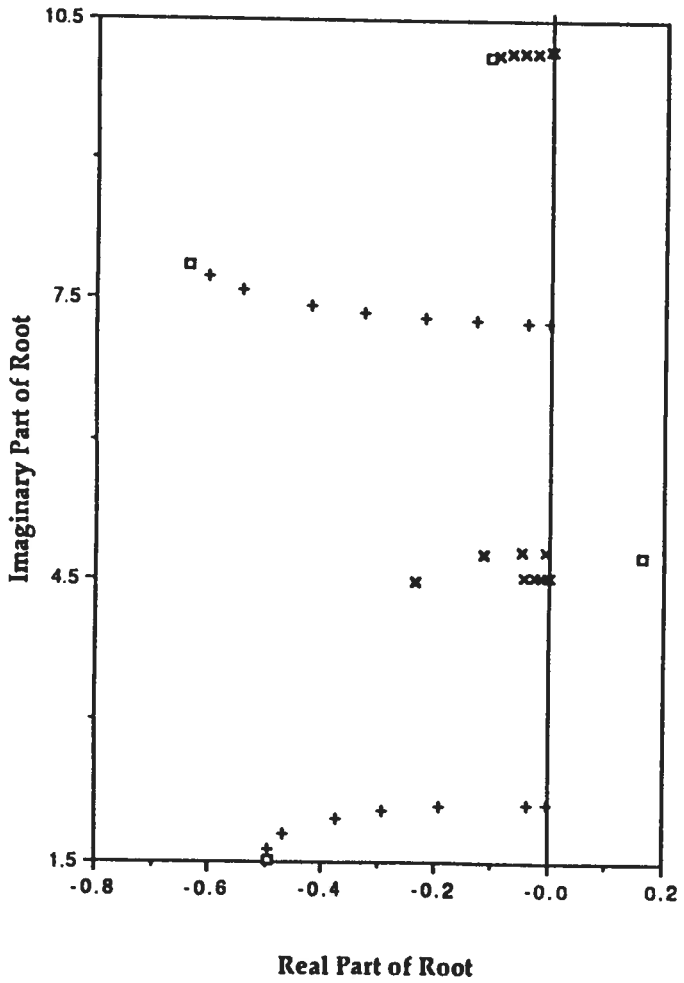

FIG. 2c. Velocity-feedback control for elastically restrained bar: the lowest four closed-loop poles, showing $\bar{\beta}$ for different values of μ. Pluses and crosses indicate roots for $0 < \mu < M$. Open squares indicate roots for $\mu > M$. The system is stable for $0 < \mu < M$.

Numerical results were obtained using Mathematica for n ranging between 0 and 10, using Equations (62a) and (62c). The smallest value of μ was found to be 2.00449 for $\bar{\beta} = 59.21i$, with $n = 7$. Thus the value $M = 2$ found above is a good approximation to $\mu^{\max}$.

(b) Next we consider the same parameters as in (S1) except that $h_1 = 5$ and $h_2 = 3$. This corresponds to an elastically restrained bar. We use the

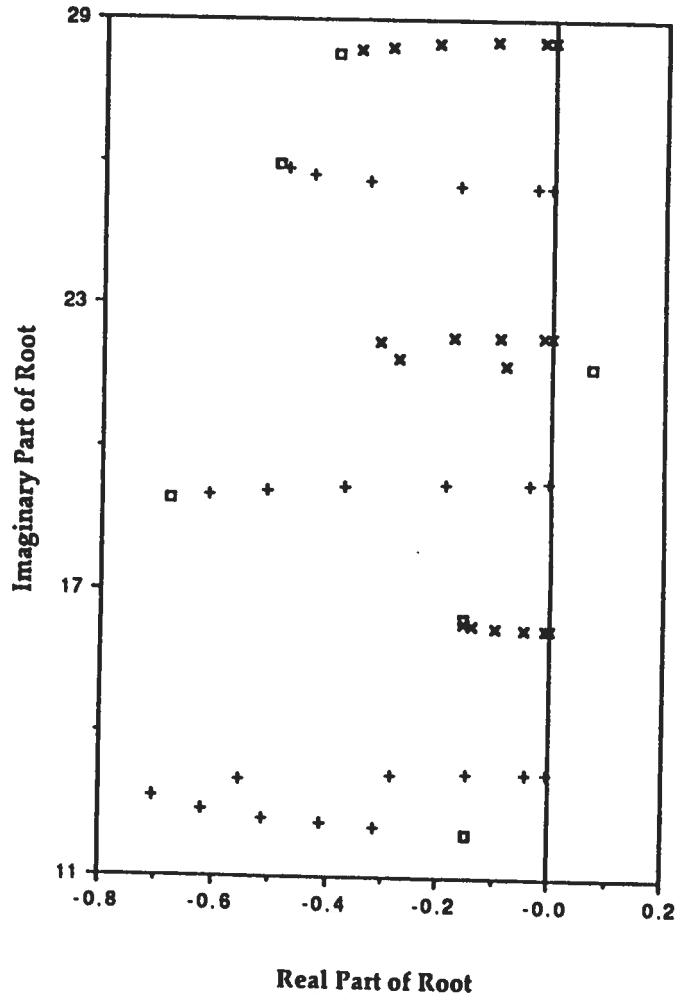

FIG. 2d. Velocity-feedback control for elastically restrained bar: the next six closed-loop poles, showing $\bar{\beta}$ for different values of μ. Pluses and crosses indicate roots for $0 < \mu < M$. Open squares indicate roots for $\mu > M$. The system is stable for $0 < \mu < M$.

control configuration C1 again. Table 2 shows the open-loop frequencies $\beta_i = \omega_i / c$ for the first ten modes of vibration. The root loci of $\bar{\beta}$ (for the upper half s-plane) are shown in Figures 2c and 2d for the lowest ten open-loop poles. As predicted by our theoretical results, as long as $0 < \mu < M = 2$, the root loci lie in the left half s-plane. The roots for values of $\mu > M$ are indicated by open squares.

TABLE 2

Mode number	β_i
1	2.1239
2	4.5556
3	7.2763
4	10.169
5	13.154
6	16.191
7	19.258
8	22.345
9	25.444
10	28.552

EXAMPLE 2 (Lead-lag compensator). Using the same parameter values as in (S1), we now take

$$\mathcal{T}_c(i\omega) = \frac{1+\frac{1}{2}i\omega}{1+\frac{1}{5}i\omega}$$

and use configuration C1. We note that the condition (58a) is satisfied. Figure 3 shows graphs of the left-hand side and right-hand side of Equation

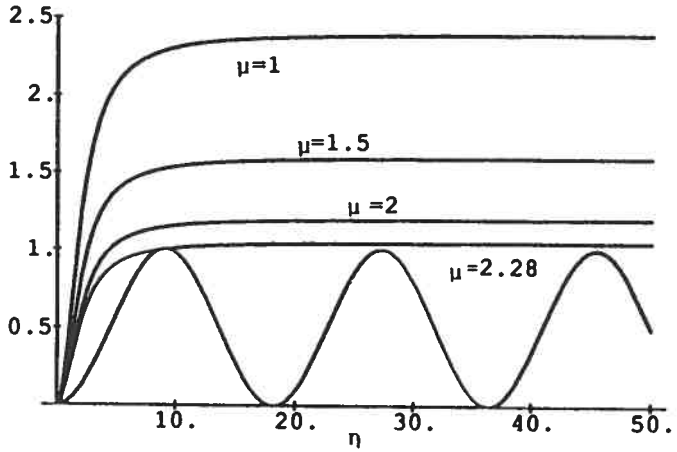

FIG. 3. Lead-lag compensator: the left-hand side of Equation (56a) and its right-hand side for different values of μ. For $0 < \mu < M = 2.28$, Equation (56a) cannot be satisfied, ensuring stability.

(56a). We see that as long as

$$\mu < \frac{\eta_1^* b(\eta_1^*)}{a^2(\eta_1^*) + b^2(\eta_1^*)} \cdot c,$$

where $\eta_1^* = \pi/(x_a - x_3)$, the root locus must be in the left half plane. The value of M is found to be (approximately) 2.2891. We note that the smaller the separation distance $x_a - x_3$, the higher the value of η_1^* and the higher

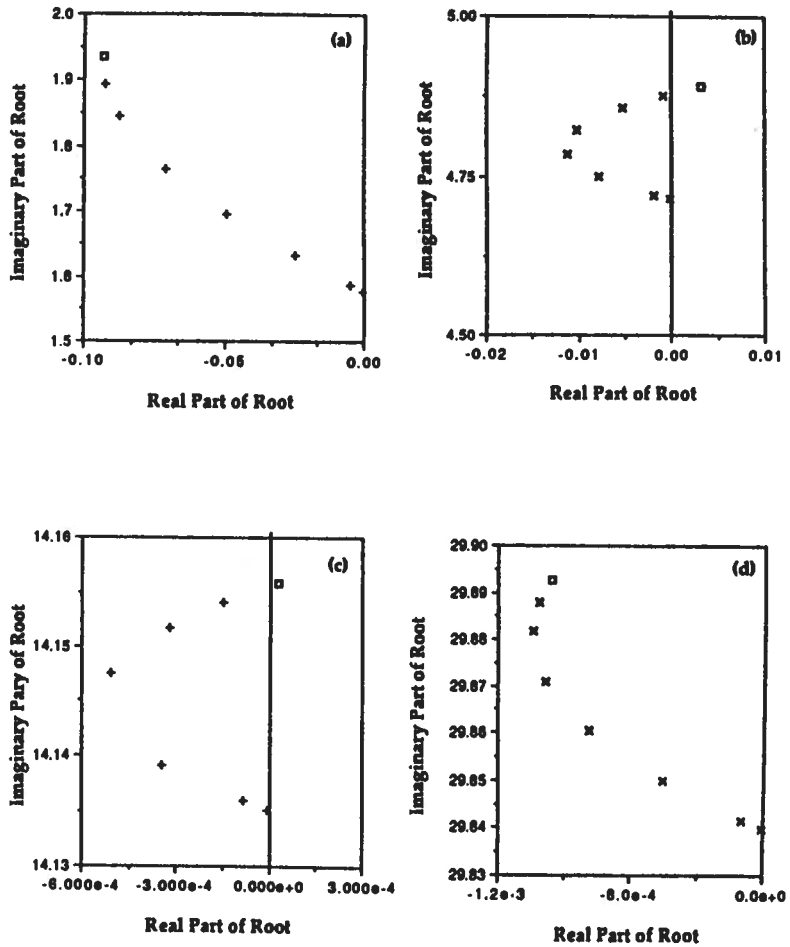

FIG. 4. Lead-lag compensator for cantilever bar: some representative closed-loop system poles, showing $\bar{\beta}$ for different values of μ. Pluses and crosses indicate roots for $0 < \mu < M$. Open squares indicate roots for $\mu > M$. The system is stable for $0 < \mu < M$.

the value of M, indicating that the closed-loop system will remain stable for larger values of the feedback gain μ. This is consistent with our results for collocated control.

The root loci are determined using different values of μ (typically $\mu = 0.01, 0.1, 0.5, 1, 1.5, 2, 2.28$, and 2.5). Again roots for values of $\mu < M$ are indicated by pluses and crosses; roots for values of $\mu > M$, by open squares. Figure 4 shows these loci for four of the roots. Note that in Figure 4(b) and (c) the root loci turn around and cross into the right half plane for $\mu = 2.5$. The roots loci for all ten roots were found to lie in the left half s-plane for $0 < \mu < M$.

VI. CONCLUSIONS

In this paper we have shown that for systems of finite extent described by the one-dimensional wave equation, it is possible to move all the poles into the left half s-plane when the sensors and actuators are noncollocated.

The basic reason for the instability of finite-dimensional noncollocated controllers lies in the fact that there is always a finite time for the signal to travel between the sensor and the actuator, this time delay eventually making it impossible to control all modes of the system. In this paper we have shown that by properly locating sensors and choosing appropriate time delays, the modal response of the system at time t at location x_a can be *exactly predicted* by measurements taken at three sensor locations at appropriate *prior times*. This is shown to be true for general boundary conditions. Further, it is shown that a total of three sensors is sufficient. It is this property of "perfect prediction" that causes the effect of the signal delay time to be obliterated, leading to the efficacy in using a finite-dimensional controller. The control design offered in this paper is different from those proposed in the past (e.g. see [9, 4, 2, 5]) in that we use time-delayed inputs to the controller. It is this new feature, which is motivated by our understanding of the physics of the system, which appears to be important in bringing about stability of the closed-loop system, using finite-dimensional controllers. A simple closed-form expression for the determination of the closed-loop poles using Mathematica has been provided.

This paper provides explicit bounds on the controller gains for damping out all modes. These bounds are provided in a form that can be easily calculated. More importantly, they are expressed in terms of the actual locations of the sensors and the actuators. Treating collocated controller designs as special cases of noncollocated designs, previously obtained results are put in a more general framework. Simulation results are presented validating the control design methodology as well as the theoretically obtained bounds on the controller gains.

The cost of noncollocation is shown to be *at most* an additional two sensors. For systems with one end fixed, the cost is one additional sensor; for a fixed-fixed system, control can be gained through the use of just one noncollocated sensor. We note that the general three-sensor situation yields two different configurations vis-à-vis the location of the actuator. We have shown that through the proper placement of such sensors, noncollocated control using simple controllers leads to no spillover effects. The fact that complete controllability is achieved is due to the ability to predict the modal response from time-delayed responses at other locations on the system.

The fact that finite-dimensional, simple controllers can be used to control neutrally stable distributed systems with noncollocated sensors and actuators is a result which will have wide application in many areas of mechanical control as well as the control of large space structures. Such methods could be extended to general distributed-parameter systems which model structural, mechanical, and aerospace systems.

APPENDIX 1

We show here that the poles of the transfer function G_{cl} are indeed given by the equation

$$\det A = 0,$$

where A is defined in Equation (39). [Note that we assume that the controller has no zeros on the imaginary axis, i.e., that $K(i\omega) \neq 0$ for all ω.] For this result to be true, it is enough to show that when $\mu \neq 0$, the closed-loop poles of G_{cl} cannot occur at the open-loop poles of $g_0(x, \xi, s)$.

LEMMA 1. *In the vicinity of any open-loop pole, $\pm i\omega_j$, the open-loop transfer function $g_0(x, \xi, s)$ can be expressed as*

$$g_0(x, \xi, s) = A(x, \xi, s) + \frac{u_j(x)u_j(\xi)}{N_j(s^2 + \omega_j^2)}, \tag{A.1}$$

where $A(x, \xi, s)$ is analytic in the vicinity of $s = \pm i\omega_j$.

PROOF. Noting Equations (17) and (18), the result follows. ∎

LEMMA 2. *In the vicinity of any open-loop pole, $\pm i\omega_j$, the function $J(\xi)$ defined in Equation (36) can be expressed as*

$$J(\xi) = B + \frac{u_j(\xi)}{N_j\left(s^2+\omega_j^2\right)}\left[u_j(x_1)e^{-sT_1} - u_j(x_2)e^{-sT_2} + u_j(x_3)e^{-sT_3}\right], \tag{A.2}$$

where B is analytic in the vicinity of $s = \pm i\omega_j$.

PROOF. Using (A.1) we get

$$g_0(x_i,\xi,s)e^{-sT_i} = A_i(x_i,\xi,s) + e^{-sT_i}\frac{u_j(x_i)u_j(\xi)}{N_j\left(s^2+\omega_j^2\right)}, \qquad i = 1,2,3. \tag{A.3}$$

The result follows with $B = A_1 + A_2 + A_3$.

LEMMA 3. *The quantity $g_0(x,x_a,s)J(\xi)$ can be expressed as*

$$\left\{R_1 + \frac{u_j(x)u_j(x_a)}{N_j\left(s^2+\omega_j^2\right)}\right\} \times \left\{R_2 + \frac{u_j(\xi)}{N_j\left(s^2+\omega_j^2\right)}\left[u_j(x_1)e^{-sT_1} - u_j(x_2)e^{-sT_2} + u_j(x_3)e^{-sT_3}\right]\right\}, \tag{A.4}$$

where R_1 and R_2 are analytic at $s = \pm i\omega_j$.

PROOF. The result is obvious from (A.2) and (A.3).

LEMMA 4. *The quantity $g_0(x,\xi,s)J(x_a)$ can be expressed as*

$$\left\{R_3 + \frac{u_j(x)u_j(\xi)}{N_j\left(s^2+\omega_j^2\right)}\right\} \times \left\{R_4 + \frac{u_j(x_a)}{N_j\left(s^2+\omega_j^2\right)}\left[u_j(x_1)e^{-sT_1} - u_j(x_2)e^{-sT_2} + u_j(x_3)e^{-sT_3}\right]\right\}, \tag{A.5}$$

where R_3 and R_4 are analytic at $s = \pm i\omega_j$.

PROOF. Same as above. ∎

RESULT A.1. *Consider any pole of the open-loop transfer function, say $\pm i\omega_j$. When $\mu \neq 0$, the closed-loop poles of G_{cl} cannot be at $s = \pm i\omega_j$.*

PROOF. The closed-loop transfer function can be written as

$$G_{cl} = \frac{g_0(x,\xi,s) - \mu\mathscr{T}_c(s)\left[g_0(x,x_a,s)J(\xi) - g_0(x,\xi,s)J(x_a)\right]}{1 + \mu T_c(s)J(x_a)}. \tag{A.6}$$

We next do the following: (1) substitute in the numerator of (A.6) for $g_0(x,x_a,s)J(\xi)$ and $g_0(x,\xi,s)J(x_a)$ using (A.4) and (A.5), (2) multiply the numerator and denominator by $s^2+\omega_j^2$, and (3) take the limit of G_{cl} as $s \to \pm i\omega_j$. This yields

$$\lim_{s\to\pm i\omega_j} G_{cl} = \frac{\begin{array}{r}u_j(x)u_j(\xi) + \mu\mathscr{T}_c(\pm i\omega_j)\big[u_j(x_a)\{R_3u_j(x_a) - R_2u_j(x)\} \\ + u_j(\xi)\{R_4u_j(x) - R_1u_j(x_a)\}\big]\end{array}}{\mu\mathscr{T}_c(\pm i\omega_j)u_j^2(x_a)}, \tag{A.7}$$

where we have used Equation (26) and the fact that R_1, R_2, R_3, R_4 are all analytic in the vicinity of $\pm i\omega_j$. Thus G_{cl} is bounded as $s \to \pm i\omega_j$ as long as $\mu > 0$, because x_a is not at any node of any mode. Note also that for the limit in (A.7) to be bounded, we require that $\mathscr{T}_c(i\omega_j) \neq 0$ for $j = 1, 2, \ldots$, i.e., the zeros of the controller do not lie on the imaginary axis.

Hence all the closed-loop poles are obtained as the zeros of the equation $\det A = 0$. ■

APPENDIX 2

We shall prove the relation (49) here.

The condition $\det A = 0$ leads, in the vicinity of an open-loop pole $s_k = \pm i\omega_k$, to the following expression:

$$\begin{aligned}(s^2 + \omega_k^2) + \mu \mathscr{T}_c(s) \sum_{\substack{n=1 \\ n \neq k}}^{\infty} \frac{u_n(x_a)(s^2 + \omega_k^2)}{N_n(s^2 + \omega_n^2)} \{u_n(x_1)e^{-sT_1} - u_n(x_2)e^{-sT_2} \\ + u_n(x_3)e^{-sT_3}\} \\ = -\frac{\mu}{N_k} \mathscr{T}_c(s) u_k(x_a)\{u_k(x_1)e^{-sT_1} - u_k(x_2)e^{-sT_2} + u_k(x_3)e^{-sT_3}\}.\end{aligned} \tag{A.8}$$

Differentiating (A.8) with respect to μ, and taking the limit as $\mu \to 0$, we get

$$\begin{aligned}\left.\frac{ds}{d\mu}\right|_{\mu=0} \\ = -\frac{\mathscr{T}_c(s)}{2s} \sum_{\substack{n=1 \\ n \neq k}}^{\infty} \frac{u_n(x_a)(s^2 + \omega_k^2)}{N_n(s^2 + \omega_n^2)} \\ \times \{u_n(x_1)e^{-sT_1} - u_n(x_2)e^{-sT_2} + u_n(x_3)e^{-sT_3}\} \\ - \frac{\mathscr{T}_c(s)}{s}\left[\frac{u_k(x_a)\{u_k(x_1)e^{-sT_1} - u_k(x_2)e^{-sT_2} + u_k(x_3)e^{-sT_3}\}}{2N_k}\right].\end{aligned} \tag{A.9}$$

We now take limits on both sides of the above expression as $s \to \pm i\omega_k$, and noting Equation (26), we obtain the result in Equation (49). Note that we require that $\lim_{s \to \pm i\omega_k} \mathscr{T}_c(s)/s$ exists, so that the first term on the right-hand side of (A.9) goes to zero.

APPENDIX 3

LEMMA 1. *The Green's function for Equation* (1) *for homogeneous boundary conditions is always of the form*

$$g_0(x, \xi, s) = \begin{cases} \dfrac{\sinh(\bar{\beta}\xi + \bar{\psi})\sinh(\bar{\beta}x + \bar{\phi})}{\bar{\beta}c^2 \sinh(\bar{\psi} - \bar{\phi})}, & x \leqslant \xi, \\ \dfrac{\sinh(\bar{\beta}\xi + \bar{\phi})\sinh(\bar{\beta}x + \bar{\psi})}{\bar{\beta}c^2 \sinh(\bar{\psi} - \bar{\phi})}, & x \geqslant \xi, \end{cases} \tag{A.10}$$

where $s^2 = c^2\bar{\beta}^2$.

PROOF. This result can be found using standard techniques (see [11]). ■

LEMMA 2. *When* $s = \pm i\eta$, *the Green's function can be expressed as*

$$g_0(x, \xi, i\eta) = \begin{cases} \dfrac{\sin(\beta\xi + \psi)\sin(\beta x + \phi)}{\beta c^2 \sin(\psi - \phi)}, & x \leqslant \xi, \\ \dfrac{\sin(\beta\xi + \phi)\sin(\beta x + \psi)}{\beta c^2 \sin(\psi - \phi)}, & x \geqslant \xi, \end{cases} \tag{A.11}$$

where $\bar{\psi} = i\psi$, $\bar{\phi} = i\phi$, *and* $\bar{\beta} = i\beta$ *with* $\beta = \pm \eta/c$.

PROOF. Making the necessary substitutions in (A.10), the result follows. ■

Note that β, ϕ, and ψ are all now real numbers. The expressions for ϕ and ψ for the system described by Equations (1) to (3) are given by

$$\tan\phi = \frac{\beta}{h_1} \quad \text{and} \quad \tan\psi = \frac{h_2 \sin\beta L + \beta\cos\beta L}{\beta\sin\beta L - h_2\cos\beta L}. \tag{A.12}$$

LEMMA 3. *The open-loop poles of the transfer function are located at either*

$$\bar{\psi} - \bar{\phi} = in\pi \quad or \quad \bar{\beta} = 0. \tag{A.13}$$

PROOF. The result follows from (A.10). ■

LEMMA 4. *The open-loop system* (1)–(3) *has a zero eigenvalue only if both* h_1 *and* h_2 *are zero.*

PROOF. The proof follows directly from the development of the Green's function. ■

Note that when either h_1 or h_2 is different from zero, the open-loop poles are obtained only from the relation $\bar{\psi} - \bar{\phi} = 0$. Furthermore, for such a system, zero is not an eigenvalue for the open-loop system.

LEMMA 5. *The closed-loop poles are obtained from the relation*

$$1 + \mu \mathscr{T}_c(s)\left[g_0(x_a, x_a, s) - \frac{e^{-\bar{\beta}(x_a - x_3)}}{\bar{\beta}c^2}\sinh\bar{\beta}(x_a - x_3)\right] = 0, \tag{A.14a}$$

where $x_3 < x_a < x_2 < x_1$ *and* $x_1 - x_2 = x_a - x_3$; $s^2 = c^2\bar{\beta}^2$.

PROOF. We use the expressions for the open-loop transfer function in (A.10) given by Equation (46). This yields

$$1 + \mu \frac{\mathscr{T}_c(s)}{2\bar{\beta}c^2\sinh(\bar{\psi} - \bar{\phi})}$$

$$\times\left[\cosh(2\bar{\beta}x_a + \bar{\phi} + \bar{\psi}) - e^{\bar{\psi} - \bar{\phi}} + e^{-2\bar{\beta}(x_a - x_3)}\sinh(\bar{\psi} - \bar{\phi})\right] = 0, \tag{A.15}$$

from which the result follows. ■

LEMMA 6. *The closed-loop poles are obtained from the relation*

$$1 + \mu \mathscr{T}_c(s)\left[g_0(x_a, x_a, s) - \frac{e^{-\bar{\beta}(x_2 - x_3)}}{\bar{\beta}c^2}\sinh\bar{\beta}(x_2 - x_3)\right] = 0, \tag{A.14b}$$

where $x_3 < x_2 < x_a < x_1$ *and* $x_1 - x_2 = x_a - x_3$, $s^2 = c^2\bar{\beta}^2$.

PROOF. The proof is the same as for Lemma 5. The result may also be verified directly. ■

LEMMA 7. *When* $s = \pm i\eta$, *we obtain the following relation for* det A:

$$\det A = 1 + \mu \mathscr{T}_c(\pm i\eta)\left[g_0(x_a, x_a, \pm i\eta) - \frac{\sin 2\beta(x_a - x_3)}{2\beta c^2}\right] + i\mu \mathscr{T}_c(\pm i\eta)\frac{\sin^2\beta(x_a - x_3)}{\beta c^2} = 0, \tag{A.16a}$$

where $x_3 < x_a < x_2 < x_1$, $\beta = \pm\eta/c$, *and* $x_1 - x_2 = x_a - x_3$. *The quantities* ϕ *and* ψ *are as in Lemma 2 above.*

PROOF. This follows from using (A.11) in the expression for det A in Equation (42), or by using (A.14a) directly. ■

LEMMA 8. *When* $s = \pm i\eta$, *we obtain the following relation for* det A:

$$\det A = 1 + \mu \mathscr{T}_c(\pm i\eta)\left[g_0(x_a, x_a, \pm i\eta) - \frac{\sin 2\beta(x_2 - x_3)}{2\beta c^2}\right] + i\mu \mathscr{T}_c(\pm i\eta)\frac{\sin^2\beta(x_2 - x_3)}{\beta c^2} = 0, \tag{A.16b}$$

where $x_3 < x_2 < x_a < x_1$, $\beta = \pm\eta/c$, *and* $x_1 - x_2 = x_a - x_3$.

PROOF. Same as Lemma 6. ■

RESULT A.3. *When the feedback controller's transfer function can be expressed as*

$$\mathscr{T}_c(i\omega) = \frac{K(i\omega)}{P(i\omega)} = a(\omega) + ib(\omega), \qquad \text{with} \quad \lim_{\omega \to \pm\alpha} \frac{b(\omega)}{\omega} > 0 \quad \forall \alpha, \tag{A.17}$$

the closed-loop control design can begin to go unstable only for those values of the gain μ (and frequency η) which satisfy the relations

$$\sin^2\left[\frac{\pm\eta(x_a - x_3)}{c}\right] = \frac{c}{\mu}\frac{(\pm\eta)b(\pm\eta)}{a^2(\pm\eta)+b^2(\pm\eta)} \tag{A.18a}$$

and

$$g_0(x_a, x_a, i\eta) - \frac{\sin[2(\eta/c)(x_a - x_3)]}{2\eta c} = -\frac{1}{\mu}\frac{a(\eta)}{a^2(\eta)+b^2(\eta)}. \tag{A.18b}$$

PROOF. The condition satisfied by the transfer function $\mathscr{T}_c$ is identical to Equation (51). We have proved in Appendix 2 [see Equation (49)] that for such transfer functions, for $\mu > 0$, all the poles of the closed-loop system move towards the left half s-plane.

For the system to become unstable the root locus of one of the poles must therefore cross the imaginary axis. We now show that for $\det A = 0$ to have roots on the imaginary axis, the condition (A.18) must be satisfied.

Assume that there exists at least one pole of the closed-loop transfer function which lies on the imaginary axis, say at $s = \pm i\eta$. We therefore set the expression (A.16) to zero. Using (A.16a), the condition (A.18a) requires

that

$$\sin^2\left[\frac{\pm\eta(x_a - x_3)}{c}\right] = \frac{c(\pm\eta)b(\pm\eta)}{\mu\left[a^2(\pm\eta)+b^2(\pm\eta)\right]} = \frac{c}{\mu}\cdot\eta\cdot\frac{\operatorname{Im}\mathscr{T}_c(i\eta)}{\|\mathscr{T}_c(i\eta)\|^2}. \tag{A.19}$$

Note that c and μ are always positive.

Thus we have shown that once the root locus for any pole begins to move towards the left half of the s-plane, for it to turn around and cross the imaginary axis again, the condition (A.19) needs to be satisfied. Note that the condition is necessary but not sufficient. ■

RESULT A.4. *A result similar to* A.3 *is valid when* $x_3 < x_2 < x_a < x_1$, $\beta = \pm\eta/c$ *and* $x_1 - x_2 = x_a - x_3$.

PROOF. Along the same lines as for Result A.3, an expression similar to (A.18) is obtained, except that on the right-hand side $x_a - x_3$ is replaced by $x_2 - x_3$. ■

LEMMA 9. *When only velocity-feedback control is used [see Equation (52)], the control cannot become unstable for any value of μ less than c.*

PROOF. As long as the condition (A.18) is not satisfied for any value of η, the control cannot become unstable. Here, $a(\omega) = 0$, and $b(\omega)/\omega$ is unity for all ω. The relation (A.18) then yields

$$\sin^2\left[\frac{\pm\eta(x_a - x_3)}{c}\right] = \frac{c}{\mu}, \tag{A.20}$$

which can never be satisfied if c/μ is greater than unity. Hence the result. ■

LEMMA 10. *When zero is not an eigenvalue of the open-loop system, for the system described by Equations* (1) *to* (3), *we have*

$$\lim_{s \to 0} g_0(x_a, x_a, s) = \frac{[1 + h_1 x_a][1 + h_2(L - x_a)]}{c^2[h_1 + h_2 + h_1 h_2 L]}. \qquad (A.21)$$

PROOF. Using the expressions in (A.11) and (A.12), and taking the appropriate limit, the result follows. Note that if both $h_1, h_2 = 0$, the Green's function at $s = 0$ is unbounded because zero is an eigenvalue of the open-loop system. ■

REFERENCES

1 T. Bailey and J. Hubbard, Distributed piezoelectric-polymer active vibration control of a cantilever beam, *J. Guidance and Control* 8(5):605–611 (Sept.–Oct. 1985).

2 M. Balas, Feedback control of linear distributed parameter systems: What can be accomplished with a finite-dimensional controller?, in *Proceedings of the IFAC Plenary Lecture, Symposium on Large Scale Systems*, Warsaw, 1983.

3 M. Balas and C. R. Johnson, Adaptive control of distributed parameter systems: The ultimate reduced order problem, in *Proceedings of the 18th IEEE Control and Decision Conference*, Ft. Lauderdale, Fla., 1979.

4 M. Balas, Feedback control of flexible systems, *IEEE Trans. Automat. Control* AC-23(4):673–679 (1978).

5 M. Balas, in *Proceedings of the NASA Workshop on Identification and Control of Flexible Space Structures*, JPL Publication 85-29, Vol. 2, 1985, pp. 111–132.

6 M. Balas, Direct velocity feedback control of large space structures, *J. Guidance and Control* 2(3):252–253 (June 1979).

7 A. G. Butkovskiy, *Structural Theory of Distributed Systems*, Ellis Horwood, New York, 1983.

8 C. A. Desoer and M. Vidyasagar, *Feedback Systems: Input-Output Properties*, Academic, 1975, pp. 182–187.

9 J. S. Gibson, An analysis of optimal modal regulation: Convergence and stability, *SIAM J. Control Optim.* 19(5):686–707 (Sept. 1981).

10 L. Meirovitch and H. Oz, Modal space control of gyroscopic systems, *J. Guidance and Control* 3(2):140–150 (1980).

11 I. Stackgold, *Green's Functions and Boundary Value Problems*, Wiley, 1979.

12 B. Yang, Personal communication. The use of two sensors for the special fixed-free boundary condition was communicated by Yang to the author. This corresponds to the special case where $\phi_n = 0$ in Equation (21).

13 B. Yang and C. D. Mote, Vibration Control of Band Saws: Theory and Experiment, Report, Dept. of Mechanical Engineering, Univ. of California, Berkeley, 1989.

14 F. E. Udwadia, Control of continuous systems, in *Proceedings of the XVth SECTAM Conference*, Atlanta, 23–25 Mar. 1990.

15 F. E. Udwadia, New methods in the intelligent control of large scale continuous systems, in *Intelligent Structures* (K. Chong, S. Liu, and J. Li, Eds.), Elsevier Science, 1990.